

**MACROCRYSTALS OF Pt-Fe ALLOY FROM THE KONDYOR PGE PLACER DEPOSIT,
Khabarovskiy Kray, Russia: TRACE-ELEMENT CONTENT,
MINERAL INCLUSIONS AND REACTION ASSEMBLAGES**

GALINA G. SHCHEKA[§]

Far East Geological Institute, Russian Academy of Sciences, 159, prospect 100-letya, Vladivostok, 690022, Russia

BERND LEHMANN, EIKE GIERTH AND KARSTEN GÖMANN

*Institute of Mineralogy and Mineral Resources, Technical University of Clausthal,
Adolph-Roemer-Strasse 2a, D-38678 Clausthal-Zellerfeld, Germany*

ALEX WALLIANOS

Max-Planck Institute of Nuclear Physics, Saupfercheckweg 1, D-69000 Heidelberg, Germany

ABSTRACT

Euhedral macrocrystals of Pt-Fe alloy from the Kondyor PGE placer, Khabarovskiy Kray, eastern Siberia, Russia, have a relatively constant composition of Pt_{2.4-2.6}Fe, tin and antimony contents up to 0.3 wt.%, and an unusually low content of all PGE except Pt. The millimetric crystals contain inclusions of fluorapatite, titanite, phlogopite, magnetite, ilmenite and iron-copper sulfides. The macrocrystals have a complex gold-rich rim, with four groups of gold alloy: tetra-auricupride (the most abundant gold-bearing phase), Au-Ag (98-54 wt.% Au), Au-Ag-Cu-Pd and Au-Pd-Cu alloys. The inner part of the reaction rim hosts a variety of PGE minerals, such as stannides, antimonides and tellurobismuthides of Pd and Pt. Stannides occur as copper-bearing (taimyrite-tatyanaitite series) and copper-free compounds (atokite-rustenburgitite series). The main antimony mineral is Sn-bearing mertieite-II. Tellurobismuthides are represented by Te-rich sobolevskite and an intermediate member of the moncheite-insizwaite solid-solution series. The reaction rim also hosts several unknown phases, such as Pd₇Bi₃, Pd₃Bi, Bi₂O₃•3H₂O, and a phosphocarbonate of thorium. The coarse crystals occur in eluvial and alluvial placers within the Kondyor massif, a zoned clinopyroxenite-dunite intrusion of Paleozoic or Mesozoic age. The inclusion assemblage suggests that the macrocrystals of Pt-Fe alloy are associated with late apatite - magnetite - phlogopite clinopyroxenite bodies, and possibly formed in a late-magmatic pegmatitic environment. The Pt-Fe alloy crystals have undergone hydrothermal overprint by NaCl-rich solutions bearing gold - silver - palladium - copper, which produced a wide variety of intermetallic compounds as well as Pd-bearing intermetallic phases. The aqueous solutions also had a minor but characteristic bismuth - tin - antimony - tellurium component.

Keywords: ferroan platinum, taimyrite, tatyanaitite, atokite, rustenburgitite, sobolevskite, moncheite-insizwaite, tetra-auricupride, Alaskan-type pluton, Kondyor, Aldan Shield, Russia.

SOMMAIRE

Les macrocristaux idiomorphes d'alliage Pt-Fe, prélevés de placers à éléments du groupe du platine (EGP) de Kondyor, Khabarovskiy Kray, Sibérie orientale, en Russie, font preuve d'une composition relativement constante, Pt_{2.4-2.6}Fe, de teneurs en étain et en antimoine atteignant 0.3% (poids), et d'un niveau anormalement faible des EGP autres que le Pt. Les cristaux millimétriques renferment des inclusions de fluorapatite, titanite, phlogopite, magnétite, ilménite et de sulfures de Fe-Cu. Les macrocristaux sont entourés d'un liseré complexe riche en or, contenant quatre groupes de compositions d'alliages d'or: tétra-auricupride (l'espèce aurifère la plus répandue), Au-Ag (98-54 % Au, poids), Au-Ag-Cu-Pd et Au-Pd-Cu. La partie interne de cette bordure de réaction renferme une variété de minéraux d'EGP, par exemple des stannures, antimoniures et tellurobismuthures de Pd et de Pt. Les stannures se présentent soit combinés avec le cuivre (série taimyrite-tatyanaitite) ou non (série atokite-rustenburgitite). Le porteur principal d'antimoine est la mertieite-II stannifère. Les tellurobismuthures sont représentés par la sobolevskite riche en Te et un membre intermédiaire de la série moncheite-insizwaite. La bordure de réaction contient en plus des phases méconnues, telles Pd₇Bi₃, Pd₃Bi, Bi₂O₃•3H₂O, et un phosphocarbonate de thorium. Les macrocristaux ont été trouvés

[§] *Present address:* Institute of Mineralogy and Mineral Resources, Technical University of Clausthal, Adolph-Roemer-Strasse 2a, D-38678 Clausthal-Zellerfeld, Germany. *E-mail address:* shcheka@email.com

dans les placers éluvionnaires et alluvionnaires développés dans le massif de Kondyor, intrusion zonée à clinopyroxénite et dunite, d'âge paléozoïque ou mésozoïque. Selon l'assemblage d'inclusions, les macrocristaux d'alliage Pt–Fe sont associés avec des venues tardives de clinopyroxénite à apatite – magnétite – phlogopite, et se seraient formés dans un milieu tardimagmatique pegmatitique. Ces gros cristaux ont subi les effets d'une recristallisation hydrothermale en présence d'une saumure porteuse d'or, argent, palladium et cuivre, ce qui a produit une grande variété de composés intermétalliques, y inclus des phases intermétalliques porteuses de Pd. Les solutions aqueuses portaient aussi en quantités moindres bismuth, étain, antimoine et tellurium.

(Traduit par la Rédaction)

Mots-clés: platine ferreux, taimyrite, tatyanaïte, atokite, rustenburgite, sobolevskite, monchélite–insizwaïte, tétra-auricupride, pluton de type Alaska, Kondyor, bouclier d'Aldan, Russie.

INTRODUCTION

The Kondyor PGE placer deposit currently has a production of about 5 t PGE/year, second in Russia to the Noril'sk Ni–PGE district, with about 100 t PGE/year. The main PGM in the Kondyor deposit is Pt–Fe alloy of xenomorphic shape and of primitive cubic cell type (Nekrasov *et al.* 1994), which in the classification scheme of Cabri & Feather (1975) is isoferroplatinum. However, the Kondyor placer is also known for spectacular euhedral Pt–Fe alloy crystals, which can reach up to several cm across (Sushkin 1995, Cabri & Laflamme 1997). These coarse crystals have a face-centered cubic cell and consist of ferroan platinum (Nekrasov *et al.* 1994, Cabri & Laflamme 1997). In the following, we will use the general term of Pt–Fe alloy for both variants.

Coarse-grained Pt–Fe alloy crystals are known only from the Kondyor deposit, and have attracted much attention from mineral collectors (Fehr *et al.* 1995, Gebhard & Schlüter 1996, Weiss *et al.* 2002) and scientists alike (Mochalov 1994, Sushkin 1995, Nekrasov *et al.* 1994, 1997, 1999, Cabri & Laflamme 1997).

An intriguing feature of the macrocrystals of Pt–Fe alloy, *i.e.*, crystals whose diameter exceeds 1.0 mm, in line with the definition of macrocrystalline rock textures: Jackson (1997, p. 382), is their unusually low content of the minor PGE elements (Nekrasov *et al.* 1994). An ion-microprobe reconnaissance study by Cabri *et al.* (1998) revealed Re and Os concentrations below the limits of detection in one large crystal (<<1 ppm Os).

Another feature of the Kondyor deposit is the large spectrum of mineral inclusions and alteration-induced minerals associated with the large crystals of Pt–Fe alloy. We describe here the mineral-inclusion and mineral-reaction assemblage of some macrocrystals, taken from the original collection of the Far East Geological Institute (FEGI), Vladivostok, Russia, and report some compositional data.

GEOLOGICAL SETTING

The Kondyor PGE placer deposit is located in the southern part of the Precambrian Aldan Shield (Ajano–

Maiskiy region of Khabarovskiy Kray), eastern Siberia (Fig. 1). The deposit is genetically related to the zoned ultramafic–alkaline Kondyor intrusion, of Uralian–Alaskan type. The concentrically zoned perfectly circular massif, 6 km across, has a dunitic core and external rings of pyroxenite, peridotite and diorite (Fig. 2). Apatite – magnetite – biotite clinopyroxenite with veins of Ti-bearing magnetite is located in the southwestern part of the massif (Sushkin 1995). Dunites and host rocks are penetrated by veins and veinlets of Mesozoic alkaline rocks, accompanied by contact-related and metasomatic transformations (Emelynenko *et al.* 1989).

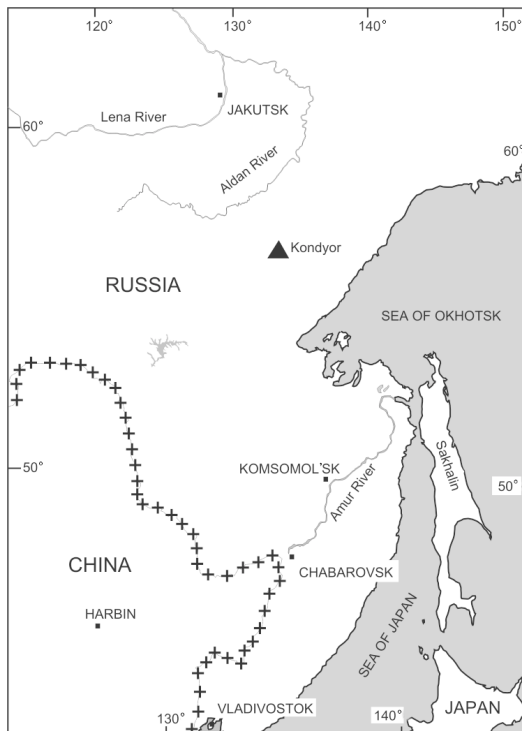


FIG. 1. Location map of the Kondyor deposit.

The Kondyor massif intrudes Archean and Proterozoic metasedimentary rocks of the Siberian Platform. The age of the intrusion is not well constrained. Parallel studies by Malitch & Thalhammer (2002) and by Pushkarev *et al.* (2002) defined the osmium isotope composition of inclusions of Os-Ir alloy in xenomorphic

Pt-Fe alloy and found a $^{187}\text{Os}/^{188}\text{Os}$ ratio of 0.1250 ± 0.002 ($n = 5$), which gives a mantle model age of 330 ± 30 Ma. Biotite from cross-cutting dikes yielded an $^{40}\text{Ar}/^{39}\text{Ar}$ age of 120 ± 1 Ma (data by G.K. Czamanske, given in Cabri *et al.* 1998). Pushkarev *et al.* (2002) found K-Ar ages of biotite of 132 ± 8 Ma and 115 ± 6 Ma for

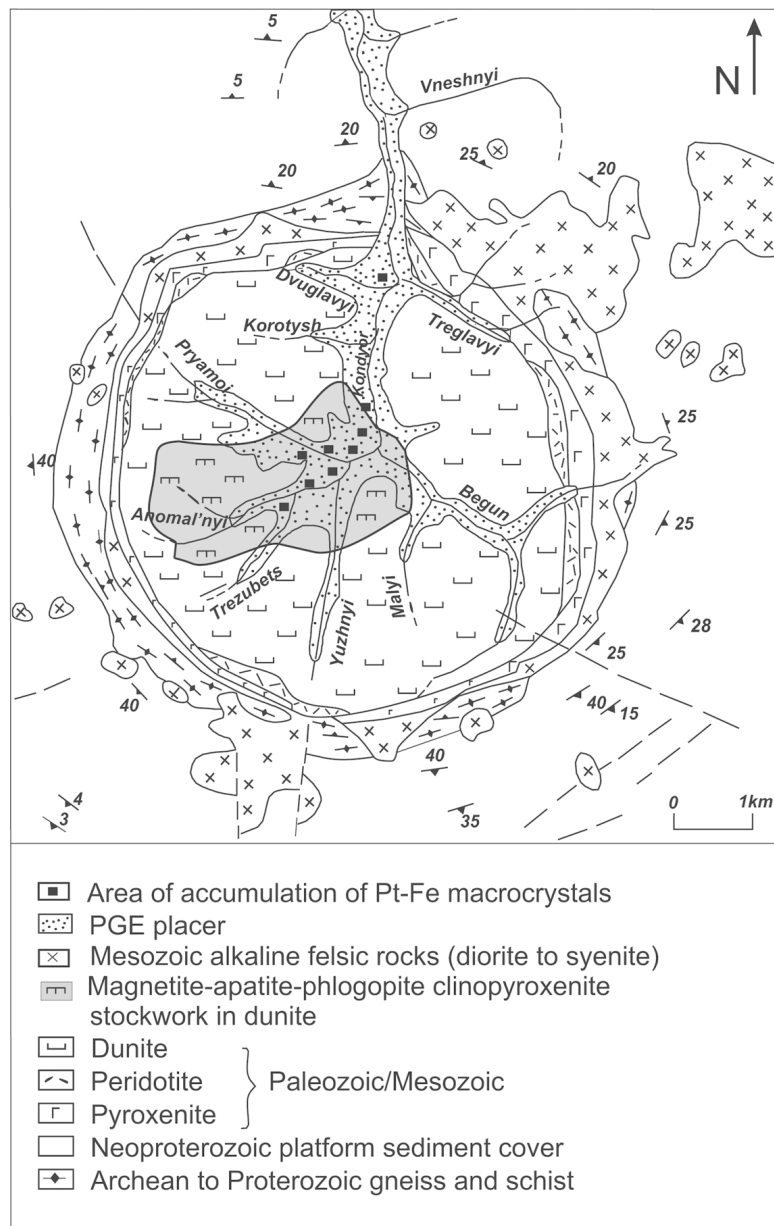


FIG. 2. Geological map of the Kondyor deposit (modified from Sushkin 1995). Note the occurrence of coarse crystals of Pt-Fe alloy in the outcrop area of the magnetite – apatite – phlogopite clinopyroxenite.

ultramafic and gabbro units, respectively, and a discordant Rb–Sr age of 123 ± 2 Ma for pyroxenite and 93 ± 47 Ma for gabbro pegmatite, respectively.

Alluvial PGM placers developed inside the intrusion in areas with a basin morphology, along the northern valley of the Kondyor River and its tributaries (Sushkin 1995). The main metal resources are concentrated in flood-plain placers with 1–1.5 m, and up to 7 m in thickness (Malitch 1999). Exploitation of the placers began in 1984 by the Amur mining company. About 40% of the total resource of around 60 t PGE have been mined so far; the average ore grade is 1.6 g PGE/m³, decreasing from 4 g/cm³ in drainages within the intrusive body to 0.5 g/m³ at its downstream extremity, over a total length of about 50 km (Yakubchuk & Edwards 2002).

Platinum–iron alloy is characteristic of the Kondyor placer. Iridium–osmium alloy and gold are present as minor components. The largest nugget found at Kondyor weighs 3521 g. The Kondyor deposit belongs to the iridium–platinum type (Mochalov *et al.* 1991), with about 85% Pt, 1.7% Ir, 0.7% Os, 0.5% Pd, 0.4% Rh, 0.1% Ru, and other elements, including Au, amounting to 9% (Yakubchuk & Edwards 2002).

OCCURRENCE OF PT–FE ALLOY MACROCRYSTALS

A remarkable and very unusual mineralogical feature of the Kondyor deposit is the presence of coarse idiomorphic crystals of Pt–Fe alloy up to 1.5 cm in size. The area of confluence of the Anomal'nyi and Trezubets

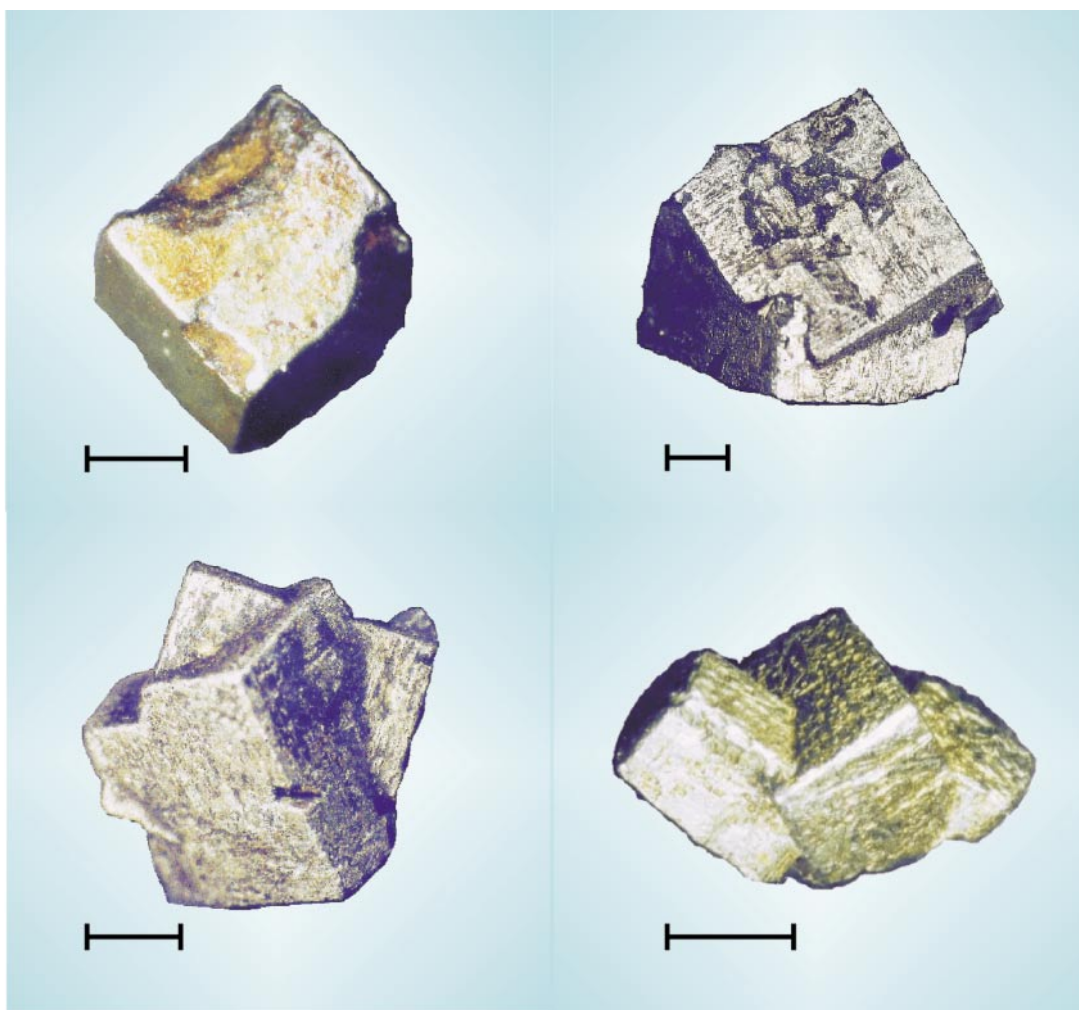


FIG. 3. Examples of coarse crystals of Pt–Fe alloy from the Kondyor placer. Scale bar is 1 mm. The yellowish tint is from gold-rich mineral assemblages.

creeks and the western bank of the Kondyor River between Pryamoi and Korotysh creeks are characterized by the occurrence of such idiomorphic crystals of Pt-Fe alloy (Fig. 2) (Sushkin 1995). The same area around Anomal'nyi Creek also shows enrichment in gold. In general, the gold content in heavy-mineral concentrates from Kondyor is about 1 wt.%, but heavy-mineral concentrates from the Anomal'nyi and Trezubets creeks have around 3–5 wt.% Au (Nekrasov *et al.* 1999).

The coarse crystals from Kondyor are hexahedral in shape. Penetration twins and intergrowth aggregates of two and more crystals are common, especially among the larger crystals (Fig. 3). The crystals commonly display a gold-rich reaction rim.

ANALYTICAL METHODS

Quantitative electron-microprobe analyses with both wavelength-dispersion and energy-dispersion X-ray spectrometry (EDS) were done with a CAMECA SX100 electron microprobe at the Institute of Mineralogy and Mineral Resources of the Technical University of Clausthal (Germany). The PGM were analyzed at 20

kV, with a beam current of 20 nA and a beam 1 μm across. The counting time varied from 10 to 30 s. The concentration of nineteen elements was determined using the following standards: FeS₂, PbTe, SnO₂, InAs and pure osmium, bismuth, ruthenium, rhodium, palladium, silver, antimony, gold, platinum, iridium, nickel, cobalt, iron and copper. The K α X-ray lines were used for Ni, Co, Fe; L α for Ru, Rh, Sn, Sb, Te, Au, Pt, Ir, Cu; L β ₁ for Pd and Ag, and M α for Os, Pb, Bi. The PdL α line was used instead of the PdL β line for the measurement of silver-bearing minerals in order to avoid the overlap of PdL β and AgL α peaks.

The following detection-limits were obtained (in wt.%): 0.15 for Os, 0.15 for Ir, 0.16 for Ru, 0.12 for Rh, 0.24 for Pd, 0.27 for Pt, 0.27 for Au, 0.32 for Ag, 0.23 for Pb, 0.04 for Fe, 0.02 for Ni, 0.09 for Cu, 0.03 for Co, 0.18 for Bi, 0.08 for Sb, 0.08 for Sn, 0.09 for Te, 0.05 for As, 0.06 for S, and 0.11 for O.

Oxides and silicates were analyzed for twelve elements using the following standards: kaersutite, Cr₂O₃ (synthetic), TiO₂, sphalerite, Fe₂O₃ (synthetic), rhodnite, forsterite (San Carlos), albite. The SiK α , KK α , CaK α , CrK α , TiK α , SK α , FeK α , MnK α , ZnK α , NaK α ,

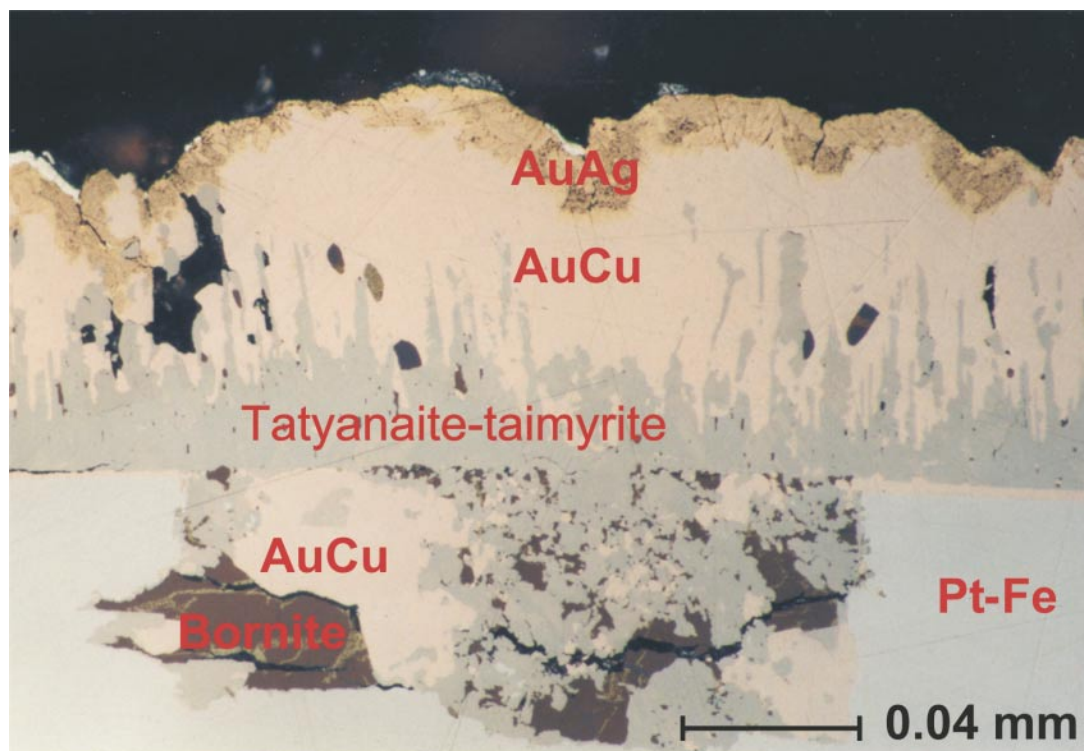


FIG. 4. Photomicrograph (oil immersion) of fine-grained intergrowth aggregate of bornite and tatyanaite-taimyrite in Pt-Fe alloy, with flame-like rim of tatyanaite-taimyrite grading outward into tetra-auricupride and overgrown by Au-Ag alloy. Sample I.

MgK α , and AlK α lines were used. The K α line of oxygen and the YAG synthetic compound have been used as a standard for oxygen in the analysis of a bismuth oxide phase.

Proton-induced X-ray emission (PIXE) analysis was done at the Heidelberg nuclear microprobe (Traxel *et al.* 1995) using incident protons at energies of 2.2 MeV and beam currents from 20 pA up to 300 pA. Calibration was done with pure elements and was checked with a number of international glass standards (Wallianos *et al.* 1997, Jochum *et al.* 2000). For data reduction, we used the GUPIX software (Maxwell *et al.* 1989, 1995).

SAMPLE DESCRIPTION AND ANALYTICAL RESULTS

Over the last two decades, the Far East Geological Institute has been actively participating in an investigation of the geology, geochemistry and mineralogy of the Kondyor deposit. A large amount of representative rocks and minerals of the Kondyor placer has been collected under the leadership of I.Ya. Nekrasov, formerly the director of the institute, in collaboration with researchers B.L. Zalishchak and V.P. Molchanov. The samples studied belong to that collection. We have chosen four alluvial euhedral crystals of Pt–Fe alloy about 2–4 mm across. They come from the Anomal'nyi Creek area (Fig. 2). The attributes of the crystals were first documented by scanning electron microscopy; polished sections were then prepared, and studied by ore microscopy and electron-microprobe analysis. In addition, a large number of xenomorphic Pt–Fe grains from a composite heavy-mineral concentrate were studied to compare their composition to that of the euhedral macrocrystals.

TABLE 1. CHEMICAL COMPOSITION OF THE FERROPLATINUM MATRIX OF THE Pt–Fe MACROCRYSTALS FROM THE KONDYOR PLACER

Sample	I <i>n</i> = 3	II <i>n</i> = 2	III <i>n</i> = 4	IV <i>n</i> = 3
Sn wt.%	0.30 ± 0.13	0.19 ± 0.04	–	0.22 ± 0.06
Sb	–	–	0.23 ± 0.10	0.11 ± 0.01
Pt	89.77 ± 0.43	88.58 ± 0.09	89.74 ± 0.78	89.01 ± 0.55
Ni	0.09 ± 0.02	0.07 ± 0	0.09 ± 0.02	0.09 ± 0.01
Fe	9.31 ± 0.04	9.04 ± 0.01	8.92 ± 0.36	9.42 ± 0.20
Cu	0.77 ± 0.13	0.60 ± 0.01	0.52 ± 0.07	0.79 ± 0.11
Total	100.23 ± 0.23	98.51 ± 0.18	99.77 ± 1.23	99.87 ± 0.67
Sn at.%	0.39 ± 0.16	0.25 ± 0.05	–	0.29 ± 0.08
Sb	–	–	0.29 ± 0.13	0.14 ± 0.01
Pt	71.57 ± 0.38	72.25 ± 0.06	72.69 ± 0.79	71.10 ± 0.54
Ni	0.23 ± 0.06	0.19 ± 0	0.23 ± 0.05	0.25 ± 0.02
Fe	25.92 ± 0.13	25.76 ± 0.09	25.27 ± 0.63	26.27 ± 0.33
Cu	1.89 ± 0.32	1.50 ± 0.03	1.32 ± 0.17	1.97 ± 0.26
Total	100	100	100	100

Note: Os, Ru, Ir, Rh, Pd, Pb, Ag, Te, Au, Co, Bi, As, S, were not detected.
–: below the detection limit of the electron microprobe used.

Sample I

Sample I is an irregular cube of 4.3 × 3.1 mm size. The crystal consists of Pt–Fe alloy with a composition of Pt_{2.5}Fe (Table 1). Copper, nickel and tin occur as minor elements. No other platinum-group elements besides Pt are detectable by electron-microprobe analysis. With reconnaissance proton-microprobe analysis, we detected zinc, germanium and antimony in the 100–1,000 ppm range (Table 2). The crystal contains 154 ppm palladium, 99 ppm rhodium, and 22 ppm ruthenium.

The crystal contains several inclusions of chromian titanian magnetite, up to 0.9 mm in size, with up to 8 wt.% TiO₂ and 3 wt.% CrO₂ (Table 3). The magnetite is altered along fractures to a titanite-like phase with a high chlorine content (2.2–7.9 wt.% Cl). The chlorine-rich rim is surrounded by perovskite (Table 4) and chlorite (Table 5). Chlorite is represented both by clinocllore and chamosite. A 10- μ m inclusion of fluorapatite was found inside a clinocllore rim (Table 4). Phlogopite is present as an inclusion inside of a grain of magnetite, surrounded by clinocllore.

The Pt–Fe alloy crystal is rimmed by a complex and irregular gold-rich zone (locally up to 0.4 mm wide) with high contents of gold, copper, platinum, palladium, bismuth and tin. The main mineral phase in the inner part of the gold-rich rim is Pd–Pt-bearing tetraauricupride [(Au,Pt,Pd)Cu] (Table 6). The outer part of the rim is formed by Au–Ag alloy of Au_{0.47}Ag_{0.52}Cu_{0.01} composition as well as by small aggregates of very pure native gold in the outermost rim (Fig. 4, Table 6).

There are flame-like composite aggregates of tatyanaite [(Pt,Pd,Cu)₃Sn] – taimyrite [(Pd,Pt,Cu)₃Sn]

TABLE 2. COMPARISON OF TRACE-ELEMENT CONCENTRATIONS IN Pt–Fe ALLOY OF MACROCRYSTALS AND XENOMORPHIC GRAINS

Element	Macrocrystals		Xenomorphic grains	
	PIXE, Sample I Concentration	LOD	EMPA, <i>n</i> = 56 Concentration	LOD
Ru	22 ± 8	15	< 1600	
Rh	99 ± 14	20	6900 ± 2900	1200
Pd	154 ± 14	25	3300 ± 2700	2400
Ni	1025 ± 84	102	2000 ± 1400	300
Cu	7287 ± 206	174	6000 ± 3000	900
Zn	367 ± 141	281	n.a.	
Ge	577 ± 107	231	n.a.	
Sn	2257 ± 54	33	< 1600	
Sb	568 ± 36	42	< 800	
Te	61 ± 27	53	< 900	
Os	< 1448		1700 ± 600	1500
Ir	< 1624		21500 ± 17200	1500
Cs	88 ± 44	73	n.a.	

The following elements were found to be below their limit of detection (LOD) with the PIXE method (in ppm): Ga (2720), As (163), Au (1270), Hg (567), Br (117), Rb (564), Sr (32), Y (24), Zr (14), Nb (21), Mo (13), Ag (126), Cd (44), In (131), Ba (164), W (2430), Re (642), Tl (253), Pb (326), Bi (3533), and U (296). Note that Cabri *et al.* (1998) found a macrocrystal from Kondyor to contain Re and Os below the SIMS detection limit (<< 1 ppm); n.a.: not analyzed.

solid solution (Table 7) within the tetra-auricupride (Fig. 4). Tatyanaite also grades outward into taimyrite or occurs as an inclusion in taimyrite (Figs. 5a, b). There are rare inclusions of rustenburgite [(Pt,Pd)₃Sn] intergrown with taimyrite-tatyanaite aggregates (Figs. 5c, Table 7).

Chalcopyrite and bornite relics are present both along the boundary between Pt-Fe alloy and the gold-bearing rim, and inside the gold rim (Fig. 4, Table 8). A complex Pd-Bi mineral assemblage occurs locally at the interface between Pt-Fe alloy and tetra-auricupride (Fig. 6). This assemblage consists of sobolevskite

[PdBi] and a heterogeneous Pd-Bi-bearing aggregate (Table 9). Interstices are filled by bismuth oxide hydrate [Bi₂O₃•3H₂O] (Table 9).

Sample II

The sample is an irregular cube of 2 × 3 mm with a matrix composition of Pt_{2.6}Fe (Table 1). It has inclusions of titanite, manganoan ilmenite, chalcopyrite-

TABLE 3. CHEMICAL COMPOSITION OF TITANIAN MAGNETITE AND ILMENITE INCLUSIONS WITHIN THE MATRIX OF Pt-Fe MACROCRYSTALS, KONDYOR MASSIF

	Titanian magnetite					Ilmenite	
	1	2	3	4	5	6	7
CaO wt.%	-	-	-	-	-	0.62	0.48
Cr ₂ O ₃	3.02	3.02	3.12	3.02	3.01	-	-
TiO ₂	7.87	8.00	7.75	7.71	7.91	50.83	50.33
Fe ₂ O ₃	49.99	57.36	57.77	58.25	57.26	1.86	1.84
FeO	32.76	26.18	25.43	25.28	25.19	37.28	37.69
MnO	1.06	1.18	1.03	1.08	0.99	5.44	5.73
MgO	2.87	2.49	3.14	3.21	3.18	0.75	0.65
Al ₂ O ₃	1.39	1.41	1.60	1.42	1.62	-	-
Total	98.95	99.65	99.84	99.96	99.16	96.78	96.72

Formulae: 1. (Fe²⁺_{1.025}Mg_{0.160}Mn_{0.034})Σ_{1.219}(Fe³⁺_{1.408}Ti_{0.222}Cr_{0.089}Al_{0.061})Σ_{1.780}O₄
 2. (Fe²⁺_{0.860}Mg_{0.132}Mn_{0.037})Σ_{1.030}(Fe³⁺_{1.577}Ti_{0.220}Cr_{0.037}Al_{0.061})Σ_{1.945}O₄
 3. (Fe²⁺_{0.772}Mg_{0.172}Mn_{0.032})Σ_{1.076}(Fe³⁺_{1.578}Ti_{0.212}Cr_{0.090}Al_{0.060})Σ_{1.948}O₄
 4. (Fe²⁺_{0.767}Mg_{0.174}Mn_{0.033})Σ_{1.074}(Fe³⁺_{1.580}Ti_{0.210}Cr_{0.087}Al_{0.061})Σ_{1.948}O₄
 5. (Fe²⁺_{0.769}Mg_{0.173}Mn_{0.033})Σ_{1.073}(Fe³⁺_{1.577}Ti_{0.217}Cr_{0.087}Al_{0.070})Σ_{1.946}O₄
 6. (Fe²⁺_{0.805}Ca_{0.017}Mn_{0.119}Mg_{0.029})Σ_{1.070}(Fe³⁺_{0.936}Ti_{0.982})Σ_{1.024}O₃
 7. (Fe²⁺_{0.818}Ca_{0.013}Mn_{0.126}Mg_{0.025})Σ_{1.068}(Fe³⁺_{0.936}Ti_{0.982})Σ_{1.018}O₃
 The proportion of FeO and Fe₂O₃ are calculated according to stoichiometry. The elements Si, P, K, S, Cl, Zn, F, Na were not detected.

TABLE 4. CHEMICAL COMPOSITION OF FLUORAPATITE AND PEROVSKITE INCLUSIONS IN Pt-Fe MACROCRYSTALS, KONDYOR MASSIF

	Apatite					Perovskite	
	1	2	3	4	5	6	7
SiO ₂ wt.%	1.03	0.56	1.03	-	0.64	0.62	-
P ₂ O ₅	42.26	40.95	40.52	43.22	42.58	41.04	-
CaO	56.11	57.44	55.35	56.79	56	56.22	41.61
Cr ₂ O ₃	-	-	-	-	-	-	0.15
TiO ₂	-	-	-	-	-	-	55.75
SO ₃	-	0.27	0.47	-	0.62	0.72	0.66
Cl	-	-	-	-	-	-	0.08
F	3.3	2.26	1.74	2.83	2.17	3.23	-
FeO	0.26	-	0.1	-	-	-	0.78
Na ₂ O	-	-	-	-	-	-	0.14
MgO	0.17	-	-	-	-	-	-
Sum	103.13	101.48	99.21	102.84	102.01	101.83	99.17
-O=F	1.39	0.95	0.73	1.19	0.91	1.36	-
Total	101.74	100.53	98.48	101.65	101.1	100.47	-

Formulae: 1. Ca_{49.554}Fe_{0.013}Mg_{0.024}(PO₄)_{3.620}(SiO₄)_{0.164}F_{1.659}
 2. Ca_{10.060}(PO₄)_{3.668}(SiO₄)_{0.192}F_{1.169} 3. Ca_{40.886}Fe_{0.014}(PO₄)_{3.716}(SiO₄)_{0.172}F_{0.917}(OH)_{0.083}
 4. Ca_{40.701}(PO₄)_{3.831}F_{1.427} 5. Ca_{40.688}(PO₄)_{3.821}(SiO₄)_{0.103}F_{1.108}
 6. Ca_{40.812}(PO₄)_{3.561}(SiO₄)_{0.101}F_{1.664} 7. (Ca_{1.034}Fe_{0.015}Na_{0.006})Σ_{1.055}(Ti_{0.972}Cr_{0.003})Σ_{1.075}O₃
 -: Below detection limit. The elements K, Mn, Zn, Al were not detected.

TABLE 5. CHEMICAL COMPOSITION OF SILICATE MINERALS IN Pt-Fe MACROCRYSTALS, KONDYOR MASSIF, RUSSIA

	Quartz	Aegirine	Aegirine-augite	Ab ₁₀₀ albite	Ab ₈₀ oligocl.	Ab ₆₀ andesine	Ortho-clase	Biotite	Titanite	Chamo-site	Clinocllore
	1	2	3	4	5	6	7	8	9	10	11
SiO ₂ wt.%	99.06	53.22	55.42	71.01	67.10	60.55	68.16	40.7	31.23	47.91	31.55
P ₂ O ₅	-	0.13	-	-	-	-	-	-	-	-	-
K ₂ O	-	-	0.83	-	0.17	0.2	14.12	7.58	-	0.68	-
CaO	-	4.18	9.14	0.18	4.10	7.25	-	-	29.23	0.13	-
Cr ₂ O ₃	-	-	0.16	-	-	-	-	0.28	-	-	0.80
TiO ₂	-	2.94	0.63	-	-	-	-	1.23	37.88	0.17	-
FeO	0.45	22.00	8.82	0.14	0.33	0.2	0.21	6.77	0.91	21.12	2.11
MnO	-	0.10	-	-	-	-	-	-	-	-	-
Na ₂ O	-	11.19	3.80	9.15	8.30	7.08	0.67	1.85	-	0.26	-
MgO	-	3.37	18.32	-	-	-	-	24.89	-	5.07	35.04
Al ₂ O ₃	-	1.80	2.46	19.2	21.77	24.39	18.37	15.59	0.77	7.98	15.14
Total	99.51	98.93	99.58	99.68	101.77	99.67	101.53	98.89	100.02	83.32	84.64

Note: The elements S, Cl, Zn, F were not detected; -: below detection limit.

bornite intergrowth aggregates and fluorapatite (Tables 3, 4, 8). A gold-rich rim zone 50 to 130 μm wide consists of tetra-auricupride [(Au,Pt,Pd)Cu] together with

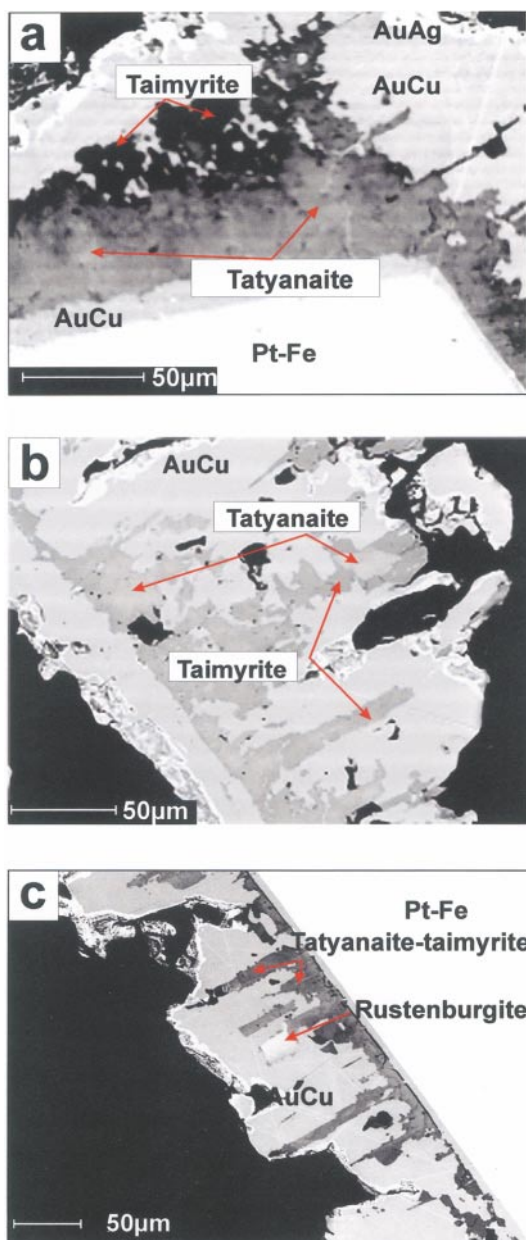


FIG. 5. Back-scattered electron images showing: a) tatyanaite grading outward into taimyrite within tetra-auricupride; b) tatyanaite inclusion in taimyrite; c) inclusions of rustenburgite intergrown with taimyrite-tatyanaite aggregates. Sample I.

TABLE 6. CHEMICAL COMPOSITION OF TETRA-AURICUPRIDE AND Au-Ag ALLOY, KONDYOR MASSIF, RUSSIA

	Tetra-auricupride				Au-Ag alloy			
	1	2	3	4	5	6	7	8
Bi wt. %	—	—	—	—	0.23	—	—	—
Pb	—	—	—	—	0.13	—	—	—
Pd	3.86	1.55	2.71	0.78	0.15	1.10	—	—
Ag	—	—	0.28	—	1.71	29.66	33.96	54.11
Au	70.76	69.55	67.31	61.50	97.92	70.43	65.63	47.34
Pt	1.87	3.91	5.33	13.91	0.15	0.00	0.30	—
Fe	—	—	0.10	0.16	—	—	—	—
Cu	25.32	24.91	25.02	24.83	—	0.44	0.27	—
Total	101.81	99.92	100.75	101.18	100.29	101.63	100.16	101.45
Bi at. %	—	—	—	—	0.21	—	—	—
Pb	—	—	—	—	0.12	—	—	—
Pd	4.51	1.88	3.19	0.93	0.28	1.59	—	—
Ag	—	—	0.33	—	3.07	42.26	48.16	67.61
Au	44.71	45.28	43.12	39.80	96.17	55.07	50.94	32.39
Pt	1.19	2.57	3.45	9.10	0.15	—	0.24	—
Fe	—	—	0.22	0.36	—	—	—	—
Cu	49.59	50.27	49.69	49.81	—	1.08	0.66	—
Total	100	100	100	100	100	100	100	100

Note: The elements Os, S, Ru, Rh, Sn, Sb, Te, Bi, Ir, Ni, Co, Fe were not detected.

TABLE 7. CHEMICAL COMPOSITION OF Pd-Pt-Cu-Sn-BEARING MINERALS, Pt-Fe MACROCRYSTALS, KONDYOR MASSIF, RUSSIA

Mineral	Pt-rich taimyrite		Tatyanaite		Rustenburgite		Atokite	
	1	2	3	4	5	6	7	8
Pd wt. %	35.86	35.57	22.24	21.87	17.42	25.27	30.94	33.84
Pt	24.72	26.47	41.96	42.22	61.42	51.55	45.29	42.70
Cu	12.31	12.10	11.40	12.23	0.84	0.59	1.03	0.59
Fe	—	—	—	0.09	—	—	0.33	—
Ni	—	—	0.13	0.09	—	—	—	0.07
Sn	25.34	25.23	22.05	21.83	19.51	20.77	21.03	21.41
Sb	0.89	0.73	0.22	0.20	0.20	0.57	0.55	0.85
Total	99.12	100.09	100.18	99.16	99.39	98.75	99.17	99.46
Pd at. %	38.37	38.03	26.35	25.59	24.89	34.38	40.01	43.28
Pt	14.43	15.44	27.12	26.95	47.87	38.26	31.95	29.79
Cu	22.07	21.66	22.61	23.97	2.01	1.34	2.23	1.26
Fe	—	—	—	0.20	—	—	0.81	—
Ni	—	—	0.28	0.19	—	—	—	0.16
Sn	24.31	24.18	23.42	22.90	24.99	25.33	24.38	24.55
Sb	0.83	0.68	0.23	0.20	0.25	0.68	0.62	0.95
Total	100	100	100	100	100	100	100	100

Formulae are calculated on the basis of 4 atoms:

1. $(\text{Pd}_{1.54}\text{Pt}_{0.58}\text{Cu}_{0.88})_{\Sigma 2.00}(\text{Sn}_{0.97}\text{Sb}_{0.03})_{\Sigma 1.00}$
2. $(\text{Pd}_{1.52}\text{Pt}_{0.62}\text{Cu}_{0.87})_{\Sigma 2.01}(\text{Sn}_{0.97}\text{Sb}_{0.02})_{\Sigma 0.99}$
3. $(\text{Pt}_{1.08}\text{Pd}_{1.05}\text{Cu}_{0.90}\text{Ni}_{0.02})_{\Sigma 2.05}(\text{Sn}_{0.94}\text{Sb}_{0.01})_{\Sigma 0.95}$
4. $(\text{Pt}_{1.08}\text{Pd}_{1.02}\text{Cu}_{0.96}\text{Fe}_{0.01}\text{Ni}_{0.01})_{\Sigma 2.06}(\text{Sn}_{0.92}\text{Sb}_{0.01})_{\Sigma 0.92}$
5. $(\text{Pt}_{1.91}\text{Pd}_{1.00}\text{Cu}_{0.08})_{\Sigma 2.99}(\text{Sn}_{1.00}\text{Sb}_{0.01})_{\Sigma 1.01}$
6. $(\text{Pt}_{1.53}\text{Pd}_{1.35}\text{Cu}_{0.05})_{\Sigma 2.96}(\text{Sn}_{1.01}\text{Sb}_{0.03})_{\Sigma 1.04}$
7. $(\text{Pd}_{1.66}\text{Pt}_{1.25}\text{Cu}_{0.09}\text{Fe}_{0.03})_{\Sigma 2.99}(\text{Sn}_{0.97}\text{Sb}_{0.03})_{\Sigma 1.00}$
8. $(\text{Pd}_{1.73}\text{Pt}_{1.19}\text{Cu}_{0.05}\text{Ni}_{0.01})_{\Sigma 2.98}(\text{Sn}_{0.96}\text{Sb}_{0.01})_{\Sigma 1.02}$

Note: The elements Os, S, Pb, Bi, Ru, Ag, Te, Ir, Co, and As were not detected; —: Below detection limit.

Pt-rich taimyrite [(Pd,Pt,Cu)₃Sn], commonly intergrown with atokite [(Pd,Pt)₃Sn] (Fig. 7). The latter occasionally forms aggregates with mertieite-II [Pd₈Sb₃] and telluroan sobolevskite [(Pd,Pt)(Bi,Te)] (Tables 9 and 10; Fig. 8a).

The tetra-auricupride has a constant palladium content of 1.4 wt.%. The platinum content varies from 6.9 up to 12.4 wt.%. A complex Au-Ag-Cu alloy with the composition of Au_{0.50}Ag_{0.36}Cu_{0.12}Pd_{0.01}Pt_{0.01} occurs as inclusions in the tetra-auricupride rim (Table 11). The outer part of the rim is formed by Au-Ag alloy of composition Au_{0.51-0.37}Ag_{0.48-0.63}Cu_{0.01} and is overgrown by pure gold [Au_{0.97}Ag_{0.03}] (Table 6). The gold-bearing rim has inclusions of anhedral quartz intergrown with albite, andesine and orthoclase as well as aegirine-augite, smectite and chamosite aggregates (Table 5).

Sample III

The sample is an irregular cube of Pt-Fe alloy [Pt_{2.6}Fe] of 4.5 × 3 mm size (Fig. 9). The crystal is affected by leaching and pervasive alteration to chamosite along crystallographic planes (001). Thin laminae of Pt-Fe alloy show contorted microdeformation (?) or dissolution fabrics. Chalcopyrite inclusions are intergrown with bornite and chalcocite. The outer part of the crystal has rounded inclusions of fractured mertieite-II, up to 0.1 mm across (Fig. 10).

The narrow gold-bearing rim, with average thickness of around 80 μm, consists of a complex Au-Ag-Cu alloy with minor palladium. The rim composition is

heterogeneous and changes from native gold [Au_{0.98}Ag_{0.02}] through Au-Ag alloy [Au_{0.49}Ag_{0.51}] to very fine-grained intergrowth aggregates of bulk composition Au_{0.66-0.68}Ag_{0.07-0.10}Cu_{0.18-0.21}Pd_{0.04-0.06} to Au_{0.69}Ag_{0.13}Cu_{0.15}Pd_{0.03}. Minor inclusions of tetra-auricupride [Au_{0.44}Cu_{0.50}Pd_{0.05}Pt_{0.01}] and atokite [(Pd,Pt)₃Sn] are present in the reaction rim.

Silicate inclusions in the gold-rich rim consist of aegirine, quartz, chamosite, clinocllore, smectite, and serpentine (Table 5).

Sample IV

The sample is a regular cube of Pt-Fe alloy [Pt_{2.4}Fe] with a crystal face of 3 mm (Fig. 11) and is characterized by a variety of sulfide inclusions. Chalcopyrite and bornite inclusions are dominant; one single inclusion (~120 μm large) of Co-bearing pentlandite was found. Several inclusions (up to 330 × 200 μm) of fluorapatite occur within the Pt-Fe matrix (Fig. 11, Table 4). Inside the fluorapatite, small (≤5 μm) rounded inclusions of an unknown Th phosphocarbonate [(Ca_{0.422}Th_{0.504}Si_{0.074})(PO₄)_{0.248}(CO₃)_{1.697}Cl_{0.055}]₂] and plumbaoan aragonite or tarnowitzite (?) [(Ca_{0.848}Pb_{0.124}Si_{0.028})CO₃] are present.

The heterogeneous gold-bearing rim is dominated by tetra-auricupride with 1.10 to 1.55 wt.% Pd and 2.67 to 10.92 wt.% Pt. Within the tetra-auricupride, there are thin aggregates (exsolution lamellae?) of Au-Ag-Cu alloy [Au_{0.48}Ag_{0.33}Cu_{0.19}]. The outer part of the rim consists of Au-Ag alloy with a composition [Ag_{0.67}Au_{0.33}].

The main PGM inclusions in the rim zone are represented by taimyrite-tatyanite solid solution (Table 7) intergrown with minerals of the moncheite-insizwaite solid solution (Fig. 8b, Table 9).

The rim zone also hosts inclusions of aegirine, chamosite and goethite.

DISCUSSION

There is a distinct difference between small xenomorphic and coarse idiomorphic Pt-Fe alloy crystals of the Kondyor massif, both in terms of chemical composition and mineral inclusions. Xenomorphic Pt-Fe alloy grains contain micro-inclusions of Ir, Ru, Os and Pt solid solutions rimmed by erlichmanite-laurite and irarsite-hollingworthite (Nekrasov *et al.* 1999). The main oxide inclusion in matrix Pt-Fe alloy is chromite. The characteristic chemical and mineralogical features of the coarse crystals are different, as noted here.

Very low abundances of PGE impurities

The PGE concentrations other than platinum are very low. Our reconnaissance proton-microprobe data indicate around 150 ppm Pd, 100 ppm Rh, and 20 ppm Ru. Osmium and iridium are below the analytical detection limit of the electron microprobe, *i.e.*, <1500 ppm. The

TABLE 8. CHEMICAL COMPOSITION OF SULFIDE INCLUSIONS IN Pt-Fe MACROCRYSTALS, KONDYOR MASSIF, RUSSIA

Mineral	Bornite		Chalcopyrite		Chalcocite		Cobalt pentlandite	
	1	2	3	4	5	6	7	8
No								
S wt. %	25.72	25.49	33.81	34.17	20.34	20.63	33.07	32.19
Fe	10.56	9.72	28.79	28.71	1.64	0.73	26.50	26.54
Cu	64.02	64.33	35.37	35.94	77.68	80.07	-	-
Ni	-	-	-	-	-	-	33.80	33.06
Co	-	-	-	-	-	-	6.25	6.36
Au	-	0.66	-	-	-	-	-	-
Pt	-	-	-	-	0.54	-	-	-
Total	100.30	100.20	97.97	98.82	100.20	101.43	99.62	98.15
S apfu	4.01	4.01	1.98	1.99	1.01	1.01	8.01	7.94
Fe	0.95	0.88	0.97	0.96	0.05	0.02	3.69	3.76
Cu	5.04	5.10	1.05	1.05	1.94	1.97	-	-
Ni	-	-	-	-	-	-	4.48	4.45
Co	-	-	-	-	-	-	0.82	0.85
Au	-	0.02	-	-	-	-	-	-
Pt	-	-	-	-	0.01	-	-	-
Σ	10	10	4	4	3	3	17	17

Note that the elements Pb, Bi, Ru, Rh, Pd, Ag, Sn, Sb, Tc, Ir, and As were not detected. -: Below detection limit.

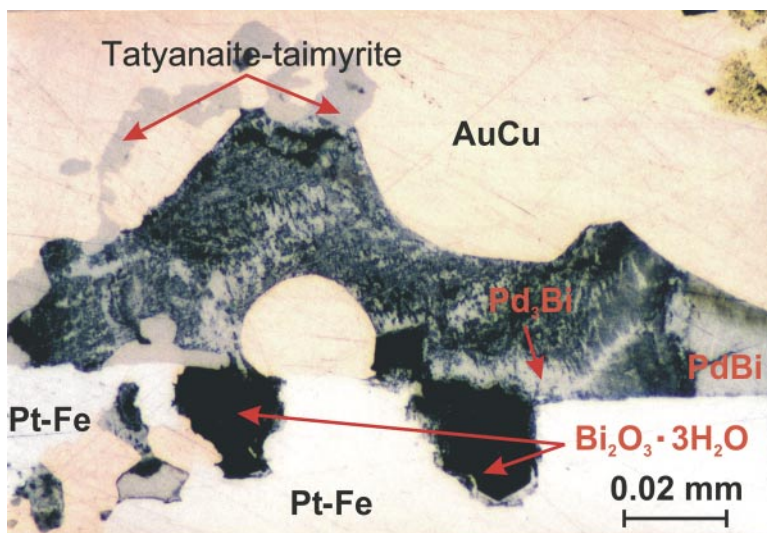


FIG. 6. Photomicrograph (oil immersion) of the complex Pd-Bi mineral assemblage at the interface between ferroplatinum and tetra-auricupride. Sample I.

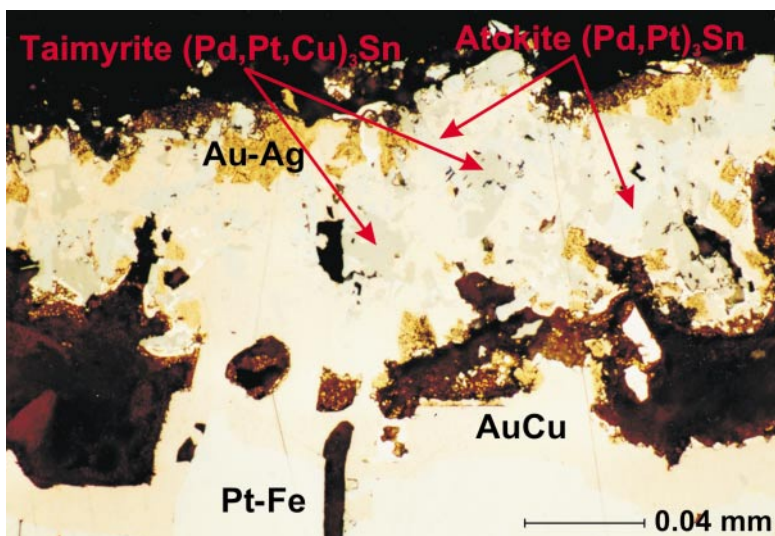


FIG. 7. Photomicrograph (oil immersion) of atokite and taimyrite intergrowth inside tetra-auricupride reaction rim on Pt-Fe alloy. Outlined section shows atokite relics within taimyrite. Sample II.

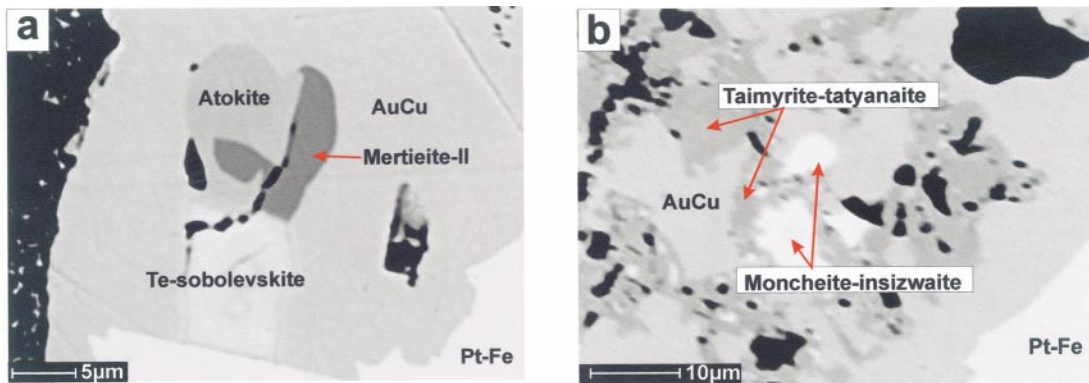


FIG. 8. Back-scattered electron images, showing a) intergrowth of atokite, mertieite-II $[\text{Pd}_8\text{Sb}_3]$ and telluroan sobolevskite $[(\text{Pd,Pt})(\text{Bi,Te})]$ within tetra-auricupride rim (sample II) and b) intergrowth of taimyrite-tatyanaitz with moncheite-insizwaite. Sample IV.

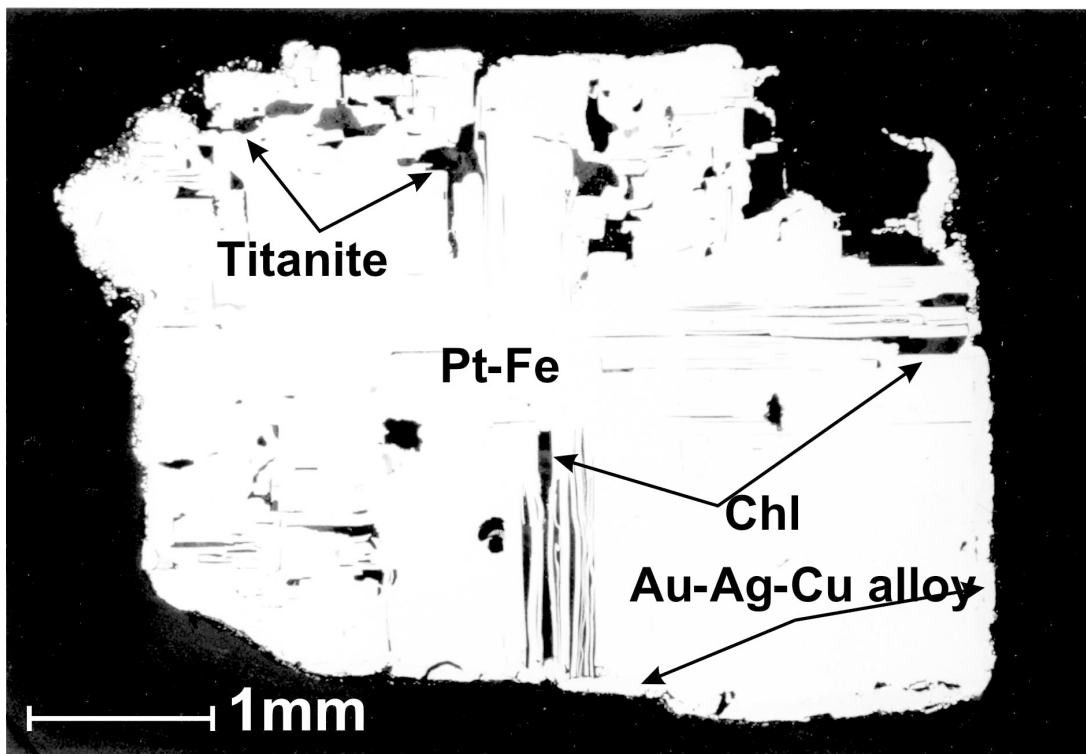


FIG. 9. Photomicrograph (oil immersion) of coarse crystal of Pt-Fe alloy with microdeformation (?) or dissolution-induced fabrics along crystallographic planes. Sample III.

earlier ion-microprobe study by Cabri *et al.* (1998) gave <<1 ppm Os.

A compilation of about 1700 compositional data on Pt-Fe alloy from about 30 occurrences worldwide shows that only 55 samples have Os values below the detection limit of electron-microprobe analysis (Cabri *et al.* 1996). However, such samples are invariably enriched in Ir, Rh, Pd and Cu. We evaluated the dataset from Cabri *et al.* (1996) with a log-normal probability graph technique, which allows limited extrapolation below detection limits. The geometric means and one standard deviation range are: 0.45 wt.% Os (0.3–1.0), 1.0 wt.% Ir (0.3–3.0), 0.07 wt.% Ru (0.02–0.2), 1.1 wt.% Rh (0.4–1.7) and 0.65 wt.% Pd (0.2–1.2). The composition of the coarse Pt-Fe alloy crystals in terms of trace elements is at least one order of magnitude lower than from all other Pt-Fe alloy occurrences (Fig. 12). We also evaluated the dataset for the xenomorphic Pt-Fe alloy from Kondyor ($n = 56$) in log-normal probability graphs. The geometric means and one standard deviation ranges

are: ~0.1 wt.% Os (<0.1–0.2), 1.2 wt.% Ir (0.1–4.5; bimodal), <<0.1 wt.% Ru, 0.6 wt.% Rh (0.45–1.2), 0.18 wt.% Pd (<0.1–0.5). These data indicate that the xenomorphic Pt-Fe alloy is relatively poor in PGE if compared to the world average, but still at least one order of magnitude richer than the macrocrystals.

Enrichment in tin and antimony

The macrocrystals studied have a composition in the range $Pt_{2.4-2.6}Fe$, with 0.66 ± 0.15 wt.% Cu, 0.07 ± 0.02 wt.% Ni, 0.11 ± 0.11 wt.% Sb, and 0.19 ± 0.11 wt.% Sn (arithmetic mean ± 1 standard deviation). The presence of the trace elements Ge, Zn, Te, and Cs at the ppm to

TABLE 9. CHEMICAL COMPOSITION OF TELLURIDE AND BISMUTHIDE INCLUSIONS IN Pt-Fe MACROCRYSTALS, KONDYOR MASSIF, RUSSIA

	Pd ₂ Bi ₂		Pd ₂ Bi		Sobolevskite		Moncheite-insizwaite		Bi oxide	
	1	2	3	4	5	6	7			
Pd wt.%	52.11	52.51	56.47	33.92	33.44	0.16	–			
Pt	2.40	1.92	2.66	2.67	4.07	36.13	1.69			
Ag	–	–	–	–	–	0.44	0.77			
Au	–	0.62	0.63	0.77	1.27	0.39	–			
Cu	0.33	–	0.15	0.20	–	–	0.15			
Bi	43.20	43.70	37.09	57.14	52.04	33.44	80.02			
Te	1.07	0.18	1.30	4.65	10.27	28.66	0.56			
Sb	0.12	–	0.23	0.64	0.53	0.24	–			
O	–	–	–	–	–	–	9.13			
							H ₂ O=7.68			
Total	99.23	98.93	98.53	99.99	101.62	99.46	100.00			
Pd at.%	67.70	68.83	71.77	48.70	46.54	0.26	–			
Pt	1.70	1.37	1.85	2.09	3.09	31.96	0.62			
Ag	–	–	–	–	–	0.70	0.51			
Au	–	0.44	0.43	0.60	0.95	0.34	–			
Cu	0.72	–	0.31	0.48	–	–	0.17			
Bi	28.58	29.16	24.00	41.76	36.87	27.62	27.30			
Te	1.16	0.20	1.38	5.57	11.91	38.77	0.31			
Sb	0.14	–	0.26	0.80	0.64	0.35	–			
O	–	–	–	–	–	–	40.67			
H	–	–	–	–	–	–	H ₂ O=30.42			
Total	100.00	100.00	100.00	100.00	100.00	100.00	100.00			

1. $(Pd_{4.77}Pt_{0.17}Cu_{0.07})_{227.01}(Bi_{2.86}Te_{0.11}Sb_{0.01})_{22.96}$; Σ atoms = 10.
 2. $(Pd_{5.85}Pt_{0.14}Au_{0.04})_{227.06}(Bi_{2.97}Te_{0.02})_{22.94}$; Σ atoms = 10.
 3. $(Pd_{2.97}Pt_{0.07}Cu_{0.01})_{22.97}(Bi_{0.96}Te_{0.06}Sb_{0.01})_{21.03}$; Σ atoms = 4.
 4. $(Pd_{0.97}Pt_{0.04}Au_{0.01}Cu_{0.01})_{21.02}(Bi_{0.24}Te_{0.12}Sb_{0.01})_{20.97}$; Σ atoms = 2.
 5. $(Pd_{0.94}Pt_{0.06}Au_{0.02})_{21.02}(Bi_{0.77}Te_{0.24}Sb_{0.01})_{20.98}$; Σ atoms = 2.
 6. $(Pt_{0.95}Ag_{0.02}Pd_{0.01}Au_{0.01})_{20.99}(Te_{1.17}Bi_{0.83}Sb_{0.01})_{22.01}$; Σ atoms = 3.
 7. $Bi_2O_3 \cdot 3H_2O$ (the amount of H_2O was calculated by difference).
- Note that the elements Rh, Os, Ru, Ir, S, Pb, Sn, Ni, Co, Fe and As were not detected. –: Below detection limit.

TABLE 10. CHEMICAL COMPOSITION OF MERTITEITE-II INCLUSIONS IN Pt-Fe MACROCRYSTALS, KONDYOR MASSIF, RUSSIA

	1			2			3		
	1	2	3	1	2	3	1	2	3
Rh wt.%	0.14	0.25	–	Rh at.%	0.15	0.26	–		
Pd	66.33	66.52	67.57	Pd	69.27	68.81	69.59		
Sn	2.27	2.33	0.13	Sn	2.12	2.16	0.12		
Sb	27.07	27.00	28.77	Sb	24.71	24.41	25.89		
Te	0.18	0.14	0.11	Te	0.16	0.12	0.10		
Au	–	0.49	–	Au	–	0.28	–		
Pt	3.00	1.81	2.86	Pt	1.71	1.02	1.60		
Cu	0.90	1.53	1.02	Cu	1.58	2.64	1.76		
As	0.20	0.19	0.64	As	0.30	0.30	0.94		
Total	100.09	100.26	101.10	Total	100	100	100		

1. $(Pd_{7.02}Pt_{0.19}Cu_{0.17}Rh_{0.02})_{28.00}(Sb_{2.72}Sn_{0.23}As_{0.03}Te_{0.02})_{23.00}$
2. $(Pd_{7.57}Pt_{0.11}Cu_{0.29}Rh_{0.03}Au_{0.03})_{28.03}(Sb_{2.69}Sn_{0.24}As_{0.03}Te_{0.01})_{22.97}$
3. $(Pd_{2.66}Pt_{0.18}Cu_{0.19})_{28.03}(Sb_{2.85}Sn_{0.01}Te_{0.01}As_{0.10})_{22.97}$

Note that the elements Fe, S, Os, Bi, Ru, Ag, Ir, and Co were not detected. –: Below detection limit.

TABLE 11. CHEMICAL COMPOSITION OF Au-Ag-Cu-Pd-Pt ALLOY IN Pt-Fe MACROCRYSTALS, KONDYOR MASSIF, RUSSIA

	1								2								3							
	1	2	3	4	5	6	7	8	1	2	3	4	5	6	7	8	1	2	3	4	5	6	7	8
Bi wt.%	–	0.54	–	–	–	–	0.78	0.93	–	–	–	–	–	–	–	–	–	–	–	–	–	–	–	–
Pd	1.69	2.62	1.54	0.73	1.45	0.69	3.95	4.29	6.96	3.16	20.32	27.18	13.08	24.87	–	0.69	–	–	–	–	–	–	–	–
Ag	–	–	–	–	–	–	–	–	–	–	–	–	–	–	–	–	–	–	–	–	–	–	–	–
Au	90.66	82.77	76.52	66.18	61.87	67.33	92.38	72.42	–	–	–	–	–	–	–	–	–	–	–	–	–	–	–	–
Pt	–	0.47	–	0.76	5.93	0.4	–	0.12	–	–	–	–	–	–	–	–	–	–	–	–	–	–	–	–
Cu	1.73	11.10	2.83	5.10	19.49	8.15	1.35	23.06	–	–	–	–	–	–	–	–	–	–	–	–	–	–	–	–
Sn	–	–	–	–	–	–	0.38	0.29	–	–	–	–	–	–	–	–	–	–	–	–	–	–	–	–
Total	101.04	100.66	101.21	99.95	101.82	101.44	98.46	101.51	–	–	–	–	–	–	–	–	–	–	–	–	–	–	–	–
Bi at.%	–	0.40	–	–	–	–	0.70	0.57	–	–	–	–	–	–	–	–	–	–	–	–	–	–	–	–
Pd	2.80	3.76	2.27	1.01	1.75	0.91	6.97	5.14	–	–	–	–	–	–	–	–	–	–	–	–	–	–	–	–
Ag	11.37	4.46	29.63	37.11	15.42	32.51	–	0.81	–	–	–	–	–	–	–	–	–	–	–	–	–	–	–	–
Au	81.05	64.28	61.08	49.49	39.96	48.21	88.01	46.91	–	–	–	–	–	–	–	–	–	–	–	–	–	–	–	–
Pt	–	0.37	–	0.58	3.87	0.29	–	0.08	–	–	–	–	–	–	–	–	–	–	–	–	–	–	–	–
Cu	4.78	26.73	7.02	11.81	39.00	18.08	3.98	46.31	–	–	–	–	–	–	–	–	–	–	–	–	–	–	–	–
Sn	–	–	–	–	–	–	0.34	0.18	–	–	–	–	–	–	–	–	–	–	–	–	–	–	–	–
Total	100	100	100	100	100	100	100	100	–	–	–	–	–	–	–	–	–	–	–	–	–	–	–	–

Note: The elements Os, S, Ru, Rh, Sb, Te, Ir, Ni, Pb, Co, Fe, and As were not detected. –: Below detection limit.

hundred ppm levels is indicated by proton-microprobe analysis. Most remarkable are the high contents of Sb and Sn, with around 2000 ppm Sn and up to 3600 ppm Sb. These two elements are consistently below the detection limit of the electron microprobe for xenomorphic Pt-Fe alloy.

Absence of Ir-, Rh-, and Os-bearing minerals

Micro-inclusions of Ir, Ru, Os and Pt solid solutions are typical of the xenomorphic Pt-Fe alloy (Nekrasov *et al.* 1999), but completely absent from the coarse Pt-Fe crystals. This mineralogical observation is reflected in the very low PGE abundances in the Pt-Fe crystals.

Absence of chromite inclusions

Chromite inclusions are typical of the xenomorphic Pt-Fe alloy and indicate a dunite affiliation (Nekrasov *et al.* 1999). Such inclusions have not been seen in the macrocrystals. Instead, fluorapatite was repeatedly observed, together with chromian titanian magnetite, titanite, manganian ilmenite, and chalcopyrite-bornite intergrowth aggregates. This mineral association is unusual for dunites, but characterizes pyroxenites and contact zones between pyroxenites and dunites (Nekrasov *et al.* 1994).

Fluorapatite inclusions

The apatite inclusions in the macrocrystals have 2–3 wt.% F and a chlorine content below the analytical detection-limit (0.05 wt.% Cl), indicating a high F/Cl environment of crystal growth, typical of evolved magmas. Fluorapatite was described as a cumulus phase from the Stillwater and Bushveld layered mafic intrusions (Boudreau *et al.* 1986). By contrast, Cl-rich apatite is typical of interstitial and vein occurrences in both intrusions and characterizes a hydrothermal environment (Boudreau *et al.* 1986). The complementary pattern of distribution of chlorine and fluorine results from the contrasting partitioning behavior of these two elements, with strong preference of Cl for aqueous fluid phases, whereas F partitions preferentially into the melt phase (Holland 1972, Manning & Pichavath 1988). Thus, the fluorapatite inclusions suggest the formation of the Pt-Fe alloy crystals in a non-hydrothermal environment, *i.e.*, in a melt system.

Hydrothermal overprint by chlorine- and alkali-rich bearing Au, Pd and base-metals-enriched fluids

The complex gold-rich rim mainly consists of four varieties of gold alloy: tetra-aurocupride, Au-Ag alloy, Au-Ag-Pd-Cu alloy, Au-Pd-Cu alloy. Tetra-aurocupride is the main gold-bearing phase, characterized by Pd (0.78–3.86 wt.%) and Pt (0.67–13.9 wt.%) contents. Gold-silver alloy has a variable composition from

native gold (97 wt.% Au) up to Au-Ag alloy (47 wt.% Au). A symplectitic intergrowth of Au-Ag-Cu-Pd alloys is typical.

Cupriferous gold is very rare in nature, and seems to be associated with hydrothermal alteration or weathering of mafic-ultramafic rocks (Knipe & Fleet 1997). The formation of tetra-aurocupride is accompanied by hydrothermal alteration of titanian magnetite to a Cl-rich titanite-like phase on fractures in titanian magnetite (Sample I), which suggests a chlorine-rich environment. The precious- and base-metal assemblage is intergrown with the hydrothermal assemblage of quartz, albite, orthoclase, andesine, as well as aegirine-augite, clinocllore, smectite and chamosite.

The secondary rim hosts a great variety of PGM phases. They are mainly represented by Pd stannides, antimonides and tellurobismuthides. Copper-bearing and Cu-free Pd stannides occur as complex zonal aggregates of tatyanaite rimmed by taimyrite and intergrown with minerals of the atokite-rustenburgite series. Genkin & Evstigneeva (1986) described a similar paragenesis at the Noril'sk complex, Russia, namely the formation of stannopalladinite (Pd,Cu)₃Sn₂ after rustenburgite (Pt,Pd)₃Sn through atokite (Pd,Pt)₃Sn. The detailed study by Barkov *et al.* (2000) of the zoned intergrowth of Pt-Pd-Cu compounds from the same occurrence shows the following sequence of crystallization: atokite → rustenburgite → tatyanaite → Pt-rich taimyrite → Pt-poor taimyrite, and inferred that this process was controlled by a decrease in temperature and increase in Cu activity. The observations on natural samples are in agreement with the experimental work of Evstigneeva & Nekrasov (1980), who studied the hydrothermal Pd-Cu-Sn-Cl system at 300–400°C and found that Pd-(Pt)-Cu stannides formed later than Cu-free compounds. A similar situation applies to the reaction assemblages studied from Kondyor. The gold-rich rim of sample II has relics of the atokite-rustenburgite series within minerals of the taimyrite-tatyanaite solid solution (Fig. 7). Sample I shows the formation of tatyanaite (Pt-rich compound) followed by later taimyrite (Pd-rich compound) (Figs. 5a, b).

Antimonides, represented by mertieite-II, generally occur as relatively large inclusions in the gold-bearing rims. Occasionally, intergrowths with atokite and telluroan sobolevskite developed along fractures (Fig. 8a). Tellurobismuthides consist of telluroan sobolevskite and an intermediate member of the moncheite-insizwaite solid solution.

CONCLUSIONS

The above observations and interpretations allow us to tentatively propose a genetic model for the formation of the Pt-Fe alloy macrocrystals. One important geological constraint is the fact that these crystals are confined to the outcrop area of apatite – magnetite – phlogopite clinopyroxenite dikes within dunite in the

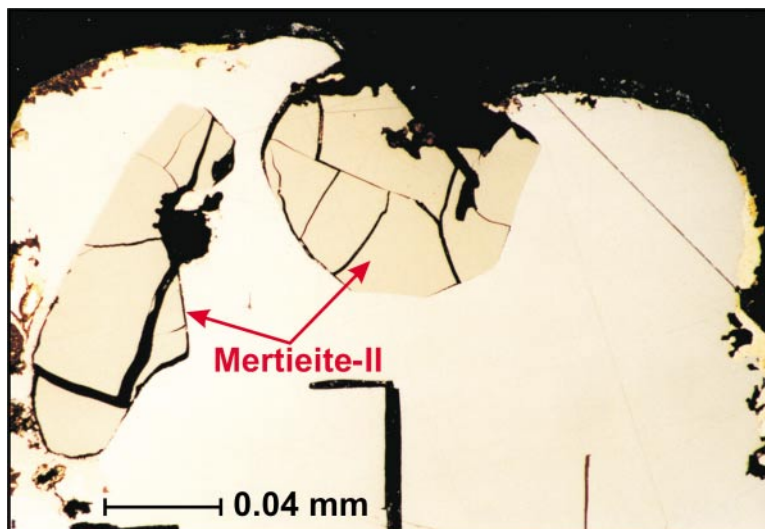


FIG. 10. Inclusions of mertieite-II in matrix of Pt-Fe alloy. Sample III (oil immersion).

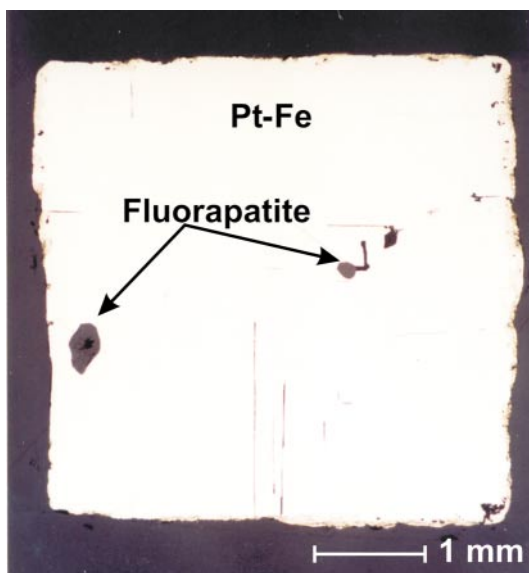


FIG. 11. Inclusions of fluorapatite in Pt-Fe alloy. Sample IV (oil immersion).

Anomal'nyy Creek and its secondary dispersion pattern (Nekrasov *et al.* 1999). The inclusion assemblage of the coarse Pt-Fe alloy crystals also suggests a petrogenetic association with the late apatite – magnetite – phlogopite clinopyroxenite bodies, but not with the dunite-dominant main intrusion. The latter is in agreement with the suggestion by Malitch & Thalhammer (2002) that

the unit-cell type of Pt_3Fe minerals depends on the host rock and that ferroan platinum is characteristic of clinopyroxenite.

The large size of the crystals could be related to crystal growth in a pegmatitic environment with a protracted magmatic evolution, *i.e.*, from residual liquids that eventually reached fluid saturation. The latter event possibly promoted the formation of miaroles or interstitial space in which coarse-grained idiomorphic PGM could form at a relatively low temperature. A similar setting applies to the Tweefontein area in South Africa, where large euhedral crystals of sperrylite up to 1.85 cm across occur in granite pegmatite and on shear zones in ironstone country-rocks of the Platreef (Wagner 1929). The coarse sperrylite crystals were interpreted as being of late-stage magmatic-hydrothermal origin (Cawthorn *et al.* 1998).

The cause of the extreme fractionation of platinum from the other PGE in the coarse Pt-Fe alloy crystals is a matter of speculation. The solubilities of Pt and Os, Ir or Rh in a sulfur-free silicate melt are not dramatically different (Borisov & Palme 1997, Borisov & Walker 2000, Ertel *et al.* 1999). However, experimental data on the partition coefficient between metal and silicate melt indicate that $D(Pt)$ is 3–4 orders of magnitude higher than $D(Os)$ at 1300–1400°C (Borisov & Walker 2000). This effect may be even larger at lower temperature and could possibly produce the huge separation of platinum from osmium (and the geochemically similar Ir, Ru, Rh). The low Pd content could be explained by the much higher solubility of Pd, compared to all other PGE, in silicate melt, similar to the solubility of Au (Borisov & Palme 1996). The Pd-Au component and base metals

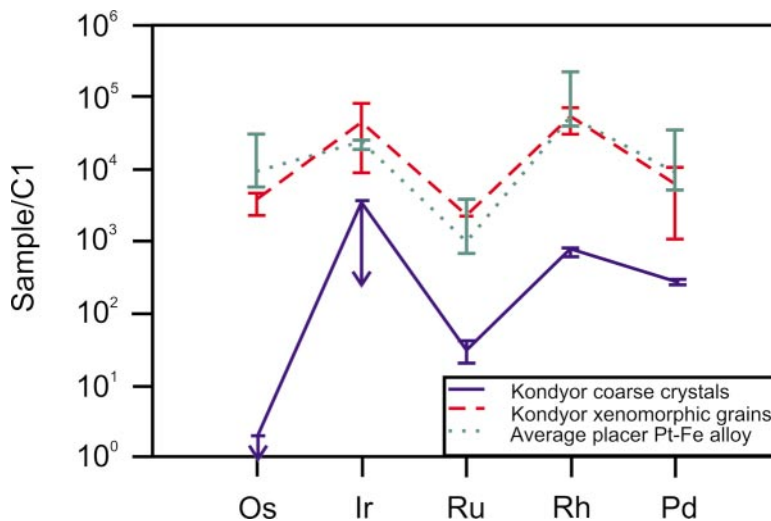


FIG. 12. Chondrite-normalized PGE distribution of euhedral macrocrystals of Pt-Fe alloy from Kondyor compared to the composition of xenomorphic grains of Pt-Fe alloy, also from Kondyor ($n = 56$) and of average placer Pt-Fe alloys ($n = 1700$) from the worldwide compilation of Cabri *et al.* (1996). Bar graphs show geometric mean ± 1 standard deviation. These parameters were generated from log-normal probability graphs, which allow limited extrapolation below the analytical detection-limit. Note that the euhedral macrocrystals from Kondyor have all PGE (except Pt) below the analytical detection-limit of the electron microprobe, but also are below the detection limit of ion-microprobe analysis for osmium (arrow) (Cabri *et al.* 1998). The Ru, Rh and Pd data are results of a proton-microprobe analysis (this study). The detection limit for Ir (arrow) is around 1500 ppm for both electron and proton microprobes.

could then be expected to fractionate into the aqueous fluid phase upon fluid saturation.

The coarse crystals of Pt-Fe alloy have undergone a hydrothermal overprint by NaCl-rich solutions bearing gold, silver, palladium and copper. This step produced intermetallic aggregates of gold-bearing alloy (tetra-aurocupride) as well as Pd-bearing intermetallic compounds. The aqueous solutions also held a minor but characteristic bismuth – tin – antimony – tellurium component. The spectrum of elements in this overprint and alteration stage is typical of late magmatic-hydrothermal fluids.

ACKNOWLEDGEMENTS

This work was supported by INTAS fellowship grant for Young Scientists YSF 00-73. The authors are very grateful to Prof. A.M. Lennikov (Far East Geological Institute) for fruitful discussion, Klaus Herrmann (Clausthal), for excellent technical support with the electron-microprobe analyses, Ulf Hemmerling for help with sample preparation, and Fred Türck (Clausthal) for computer support. We also thank Dr. Ian McDonald for his interest in this paper. We benefitted from the helpful

comments of N.D. Tolstykh and an anonymous referee, and of Robert F. Martin.

REFERENCES

- BARKOV, A.Y., MARTIN, R.F., POIRIER, G. & YAKOVLEV, Y.N. (2000): The taimyrite-tatyanaitite series and zoning in intermetallic compounds of Pt, Pd, Cu, and Sn from Noril'sk, Siberia, Russia. *Can. Mineral.* **38**, 599-609.
- BORISOV, A. & PALME, H. (1996): Experimental determination of the solubility of Au in silicate melts. *Mineral. Petrol.* **56**, 297-312.
- _____ & _____ (1997): Experimental determination of the solubility of platinum in silicate melts. *Geochim. Cosmochim. Acta* **61**, 4349-4357.
- _____ & WALKER, R.J. (2000): Os solubility in silicate melts: new efforts and results. *Am. Mineral.* **85**, 912-917.
- BOUDREAU, A.E., MATHEZ, E.A. & MCCALLUM, I.S. (1986): Halogen geochemistry of the Stillwater and Bushveld complexes: evidence for transport of the platinum-group elements by Cl-rich fluids. *J. Petrol.* **27**, 967-986.

- CABRI, J.L. & FEATHER, C.E. (1975): Platinum-iron alloys: a nomenclature based on a study of natural and synthetic alloys. *Can. Mineral.* **13**, 117-126.
- _____, HARRIS, D.C. & WEISER, T.W. (1996): Mineralogy and distribution of platinum mineral (PGM) placer deposits of the world. *Explor. Mining Geol.* **5**, 73-167.
- _____ & LAFLAMME, J.H.G. (1997): Platinum group minerals from the Konder Massif, Russian Far East. *Mineral. Rec.* **28**, 96-106.
- _____, STERN, R.A. & CZAMANSKE, G.K. (1998): Osmium isotope measurements of Pt-Fe alloy placer nuggets from the Konder intrusion using a Shrimp II ion microprobe. *Eighth Int. Platinum Symp.*, 55-57 (abstr.).
- CAWTHORN, G., LEE, C., McDONALD, I., TREDoux, M. & WHITE, J. (1998): Field excursion to the Bushveld Complex. *Excursion Guide, Eighth Int. Platinum Symp.*
- EMELYNENKO, E.P., MASLOVSKIY, A.N., ZALISHCHAK, B.L., KAMAEVA, L.V. & FOMENKO, A.S. (1989): Regularities of the location of ore mineralization at the Kondyor massif. *In Geological Conditions of the Localization of Endogenetic Ore Formation. Far Eastern Branch, Academy of Sciences, Vladivostok, Russia (100-113, in Russ.)*.
- ERTEL, W., O'NEILL, H.S.C., SYLVESTER P.J. & DINGWELL, D.B. (1999): Solubilities of Pt and Rh in haplobasaltic silicate melt at 1300°C. *Geochim. Cosmochim. Acta* **63**, 2439-2449.
- EVSTIGNEEVA, T.L. & NEKRASOV, I.YA. (1980): Synthesis conditions and phase relationships in the systems Pd-Sn-Cu-HCl and Pd₃Sn-Cu₃Sn. *In Essays of Physicochemical Petrology (V. Zharikov & V. Fed'kin, eds.)*. Nauka, Moscow, Russia (20-35, in Russ.).
- FEHR, T., HOCHLEITER, R. & WEISS, S. (1995): Sensationell: natürliche Platin-Kristalle aus Sibirien. *Lapis* **20**(10), 44-46.
- GEBHARD, G. & SCHLÜTER, J. (1996): Zvyagintsevit aus Sibirien: der erste Fund grosser Kristalle eines Palladium-Mineral. *Lapis* **21**(10), 47-48.
- GENKIN, A.D. & EVSTIGNEEVA, T.L. (1986): Association of platinum-group minerals of the Noril'sk copper-nickel sulfide ores. *Econ. Geol.* **81**, 1203-1212.
- HOLLAND, H.D. (1972): Granites, solutions and base metal deposits. *Econ. Geol.* **67**, 281-301.
- JACKSON, J.A., ed. (1997): *Glossary of Geology* (4th edition). American Geological Institute, Washington, D.C.
- JOCHUM, K.P., DINGWELL, D.B., ROCHOLL, A., STOLL, B., HOFMAN, A.W., BECKER, S., BESMEHN, A., BESSETTE, D., DIETZE, H.J., DULSKI, P., ERZINGER, J., HELLEBRAND, E., HOPPE, P., HORN, I., JANSSENS, K., JENNER, G.A., KLEIN, M., McDONOUGH, W.F., MAETZ, M., MEZGER, K., MUENKER, C., NIKOGOSIAN, I.K., PICKHARDT, C., RACZEK, I., RHEDE, D., SEUFERT, H.M., SIMAKIN, S.G., SOBOLEV, A.V., SPETTEL, B., STRAUB, S., VINCZE, L., WALLIANOS, A., WECKWERTH, G., WEYER, S., WOLF, D. & ZIMMER, M. (2000): The preparation and preliminary characterisation of eight geological MPI-DING reference glasses for in-situ microanalysis. *Geostandards Newsletter* **24**, 87-133.
- KNIFE, S.W. & FLEET, M.E. (1997): Gold-copper alloy minerals from the Kerr mine, Ontario. *Can. Mineral.* **35**, 573-586.
- MALITCH, K.N. (1999): *Platinum-Group Elements in Clinopyroxenite-Dunite Massifs of East Siberia (Geochemistry, Mineralogy, and Genesis)*. VSEGEI Press, St. Petersburg, Russia (in Russ.).
- _____ & THALHAMMER, O.A.R. (2002): Pt-Fe nuggets derived from clinopyroxenite-dunite massifs, Russia: a structural, compositional and osmium-isotope study. *Can. Mineral.* **40**, 395-418.
- MANNING, D.A.C. & PICHAVANT, M. (1988): Volatiles and their bearing on the behavior of metals in granitic systems. *In Recent Advances in the Geology of Granite-Related Mineral Deposits (R.P. Taylor & D.F. Strong, eds.)*. *Can. Inst. Mining Metall., Spec. Vol.* **39**, 13-24.
- MAXWELL, J.A., CAMPBELL, J.L. & TEESDALE, W.J. (1989): The Guelph software package. *Nucl. Instrum. Methods Phys. Res.* **B43**, 218-230.
- _____, TEESDALE, W.J. & CAMPBELL, J.L. (1995): The Guelph software package II. *Nucl. Instrum. Methods Phys. Res.* **B95**, 407-421.
- MOCHALOV, A.G. (1994): Mineralogy of platinum-group elements from dunite. *In Geology, Petrology and Ore Presence in the Kondyor Massif (Y.A. Kosigin, ed.)*. Nauka, Moscow, Russia (92-106, in Russ.).
- _____, DMITRENKO, G.G., KHOROSHILOVA, T.S. & SACHYANOV, L.O. (1991): Mineralogical-geochemical types of PGE placers and their economic significance. *In Mineralogy and Geochemistry of Placers (N.A. Shilo & N.G. Patyk-Kara, eds.)*. Nauka, Moscow, Russia (7-22, in Russ.).
- NEKRASOV, I.YA, IVANOV, V.V., LENNIKOV, A.M., SAPIN, V.I., SAFRONOV, P.P., OKTYABRSKY, R.A. & MOLCHANOVA, G.B. (1999): Native alloys of gold, copper, silver, palladium and platinum from the Kondyor alkali-ultrabasic massif. *In Geodynamics and Metallogeny*. Dalnauka, Vladivostok, Russia (in Russ.).
- _____, LENNIKOV, A.M., IVANOV, V.V., OKTYABRSKY, R.A., ZALISHCHAK, B.L. & SAPIN, B.I. (1997) Unique nature museum of new and rare minerals of precious metals. *Vestnik Dal'nevostochnogo Otdeleniya, Ross. Akad. Nauk* **3**, 135-152 (in Russ.).
- _____, _____, OKTYABRSKY, R.A., ZALISHCHAK, B.L. & SAPIN, B.I. (1994): *Petrology and Platinum Mineralization of the Alkaline-Ultramafic Ring Complexes*. Nauka, Moscow, Russia (in Russ.).
- PUSHKAREV, YU.D., KOSTOYANOV, A.I., ORLOVA, M.P. & BOGOMOLOV, E.S. (2002): Peculiarities of the Rb-Sr, Sm-

- Nd, Re-Os and K-Ar isotope systems in the Kondyor massif: mantle substratum, enriched by PGE. *Regional geology and metallogeny* **16**, 80-91 (in Russ.).
- SUSHKIN, L.B. (1995): Characteristic features of the native elements of the Kondyor deposit. *Tikhookeanskaya geologiya* **14**, 97-102 (in Russ.).
- TRAXEL, K., ARNDT, P., BOHSUNG, J., BRAUN, DULLAEUS, K.U., MAETZ, M., REIMOLD, D., SCHIEBLER, H. & WALLIANOS, A. (1995): The new Heidelberg proton microprobe: the success of a minimal concept. *Nucl. Instrum. Methods Phys. Res.* **B104**, 19-25.
- WAGNER, P.A. (1929): *The Platinum Deposits and Mines of South Africa*. Oliver and Boyd, London, U.K.
- WALLIANOS, A., ARNDT, P., MAETZ, M., SCHNEIDER, T. & TRAXEL, K. (1997): Accurate quantification resulting from precise beam monitoring and calibration. *Nucl. Instrum. Methods Phys. Res.* **B130**, 144-148.
- WEISS, S., MÖCKEL, S. & KOLESAR, P. (2002): Seltene Palladium-Mineralien und die besten Platinkristalle aus Konder, Jakutien. *Lapis* **11**, 19-27.
- YAKUBCHUK, A. & EDWARDS, A. (2002): Russia's PGM potential. *Mining Journal*, May 17, 358-359.

Received December 8, 2002, revised manuscript accepted January 22, 2004.